CORA Cork Open Research Archive
Cartlann Taighde Oscailte Chorcaí

Title	Influence of growth kinetics on Sn incorporation in direct band gap Ge1–xSnx nanowires
Authors	Doherty, Jessica;Biswas, Subhajit;Saladukha, Dzianis;Ramasse, Quentin;Bhattacharya, Tara Shankar;Singha, Achintya;Ochalski, Tomasz J.;Holmes, Justin D.
Publication date	2018-07-25
Original Citation	Doherty, J., Biswas, S., Saladukha, D., Ramasse, Q., Bhattacharya, T. S., Singha, A., Ochalski, T. J. and Holmes, J. D. (2018) 'Influence of growth kinetics on Sn incorporation in direct band gap Ge1–xSnx nanowires', Journal of Materials Chemistry C, 6(32), pp. 8738-8750. doi: 10.1039/C8TC02423E
Type of publication	Article (peer-reviewed)
Link to publisher's version	http://pubs.rsc.org/en/Content/ArticleLanding/2018/TC/C8TC02423E - 10.1039/C8TC02423E
Rights	© The Royal Society of Chemistry 2018
Download date	2024-03-29 12:52:47
Item downloaded from	https://hdl.handle.net/10468/6772



UCC
University College Cork, Ireland
Coláiste na hOllscoile Corcaigh

Electronic Supplementary Material (ESI) for Journal of Materials Chemistry C.
This journal is © The Royal Society of Chemistry 2018

Supporting Information

Influence of Growth Kinetics on Sn Incorporation in Direct Band gap $Ge_{1-x}Sn_x$ Nanowires

Jessica Doherty[1,2,3], Subhajit Biswas[1,2,3], Dzianis Saladukha[3], Quentin Ramasse[4], Tara Shankar Bhattacharya[5], Achintya Singha[5], Tomasz J. Ochalski[3], and Justin D. Holmes[1,2, 3]*

[1]School of Chemistry, University College Cork, Cork, Ireland. [2]Tyndall National Institute, University College Cork, Cork, Ireland. [3]AMBER@CRANN, Trinity College Dublin, Dublin 2, Ireland. [4]SuperSTEM Laboratory, SciTech Daresbury Campus, Daresbury WA4 4AD, United Kingdom. [5]Department of Physics, Bose Institute, Kolkata, India.

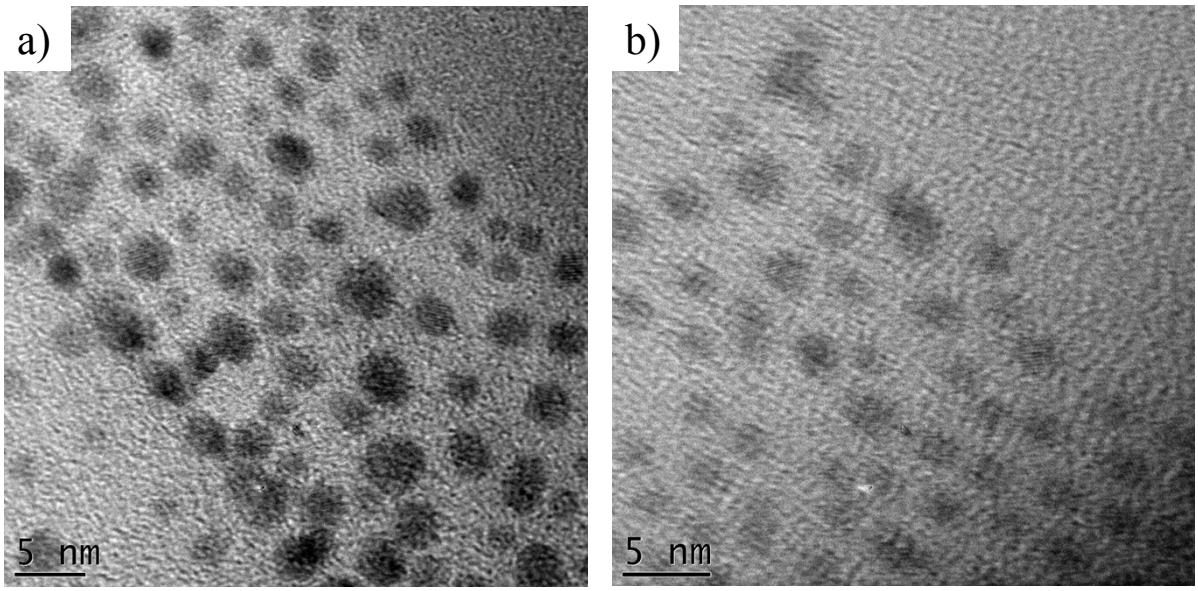


Figure S1: $Au_{1-x}Ag_x$ nanoparticles used to catalyse the growth of the $Ge_{1-x}Sn_x$ nanowires. The nanoparticles have increasing Ag content from (a) $Au_{0.90}Ag_{0.10}$ to (b) $Au_{0.80}Ag_{0.20}$ and both have a mean diameter of ~ 4-5 nm.

$$\Delta\mu = kT\ln\left(\frac{C}{C_e}\right) \ldots(Eq.\,S1)$$

Equation S1: where C is the concentration of the growth species. To lower the C_e of a growth species, a foreign species can be added to the metal seed particle which will shift the liquidus phase boundary towards a lower solute concentration.

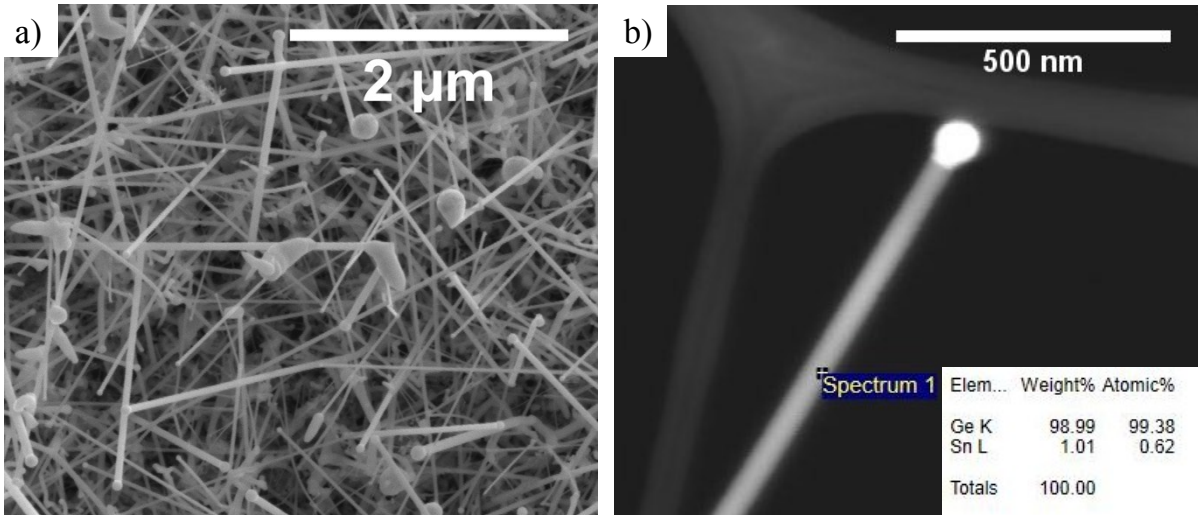


Figure S2: $Ge_{1-x}Sn_x$ nanowires grown using tetraallytin (TAT) as a Sn source. (a) depicts Sn segregation and clustering using TAT as the Sn precursor. The $Ge_{1-x}Sn_x$ nanowires grown from TAT also have a very low amount of Sn incorporation (b), with the mean Sn content of approximately 2 at. %.

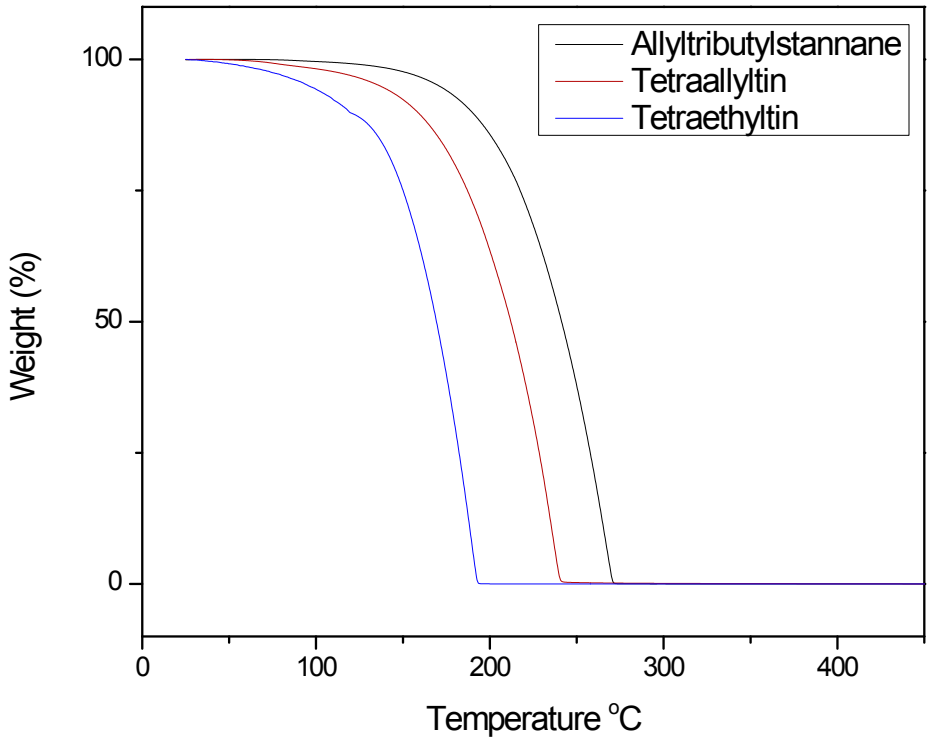


Figure S3: Thermogravimetric Analysis (TGA) of the three Sn precursors; allyltributylstanne, tetraallytin and tetraethyltin. The decomposition temperatures of these Sn molecules follows the general trend of their boiling points; ranging from TET with the lowest boiling point (181 °C at atmospheric pressure) to ATBS with the highest (353 °C at atmospheric pressure).

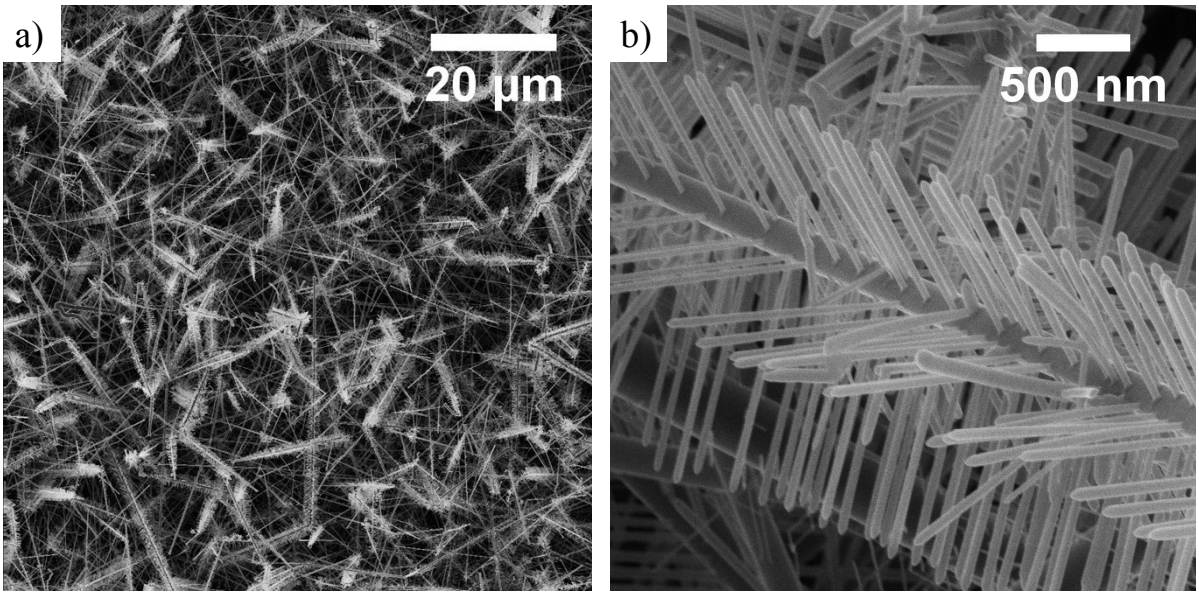


Figure S4: SEM images of the branched $Ge_{1-x}Sn_x$ nanowires grown using a specific TET concentration. The density of these branched nanowires across the substrate can be seen in (a), these branched nanowires are relatively high yield compared to the non-branched nanowires. (b) Displays the highly ordered nature of these branches, with the branch nanowires seemingly aligned along the trunk.

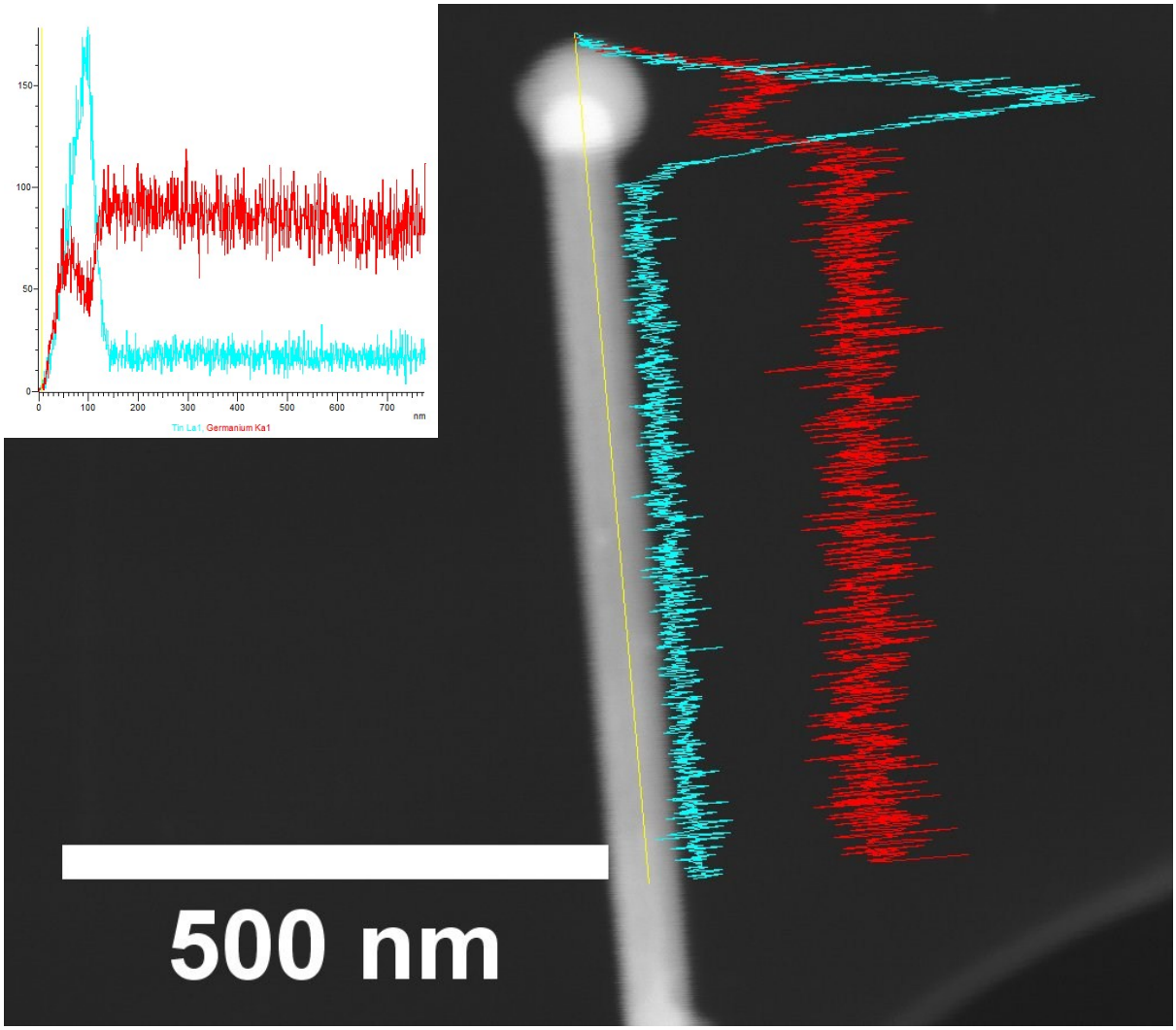


Figure S5: Linescan of EDX analysis of $Ge_{1-x}Sn_x$ nanowires with mean Sn content 8.7 at. %. In the linescan Ge is denoted by red and Sn by blue. The Sn rich nature of the seed is clearly apparent.

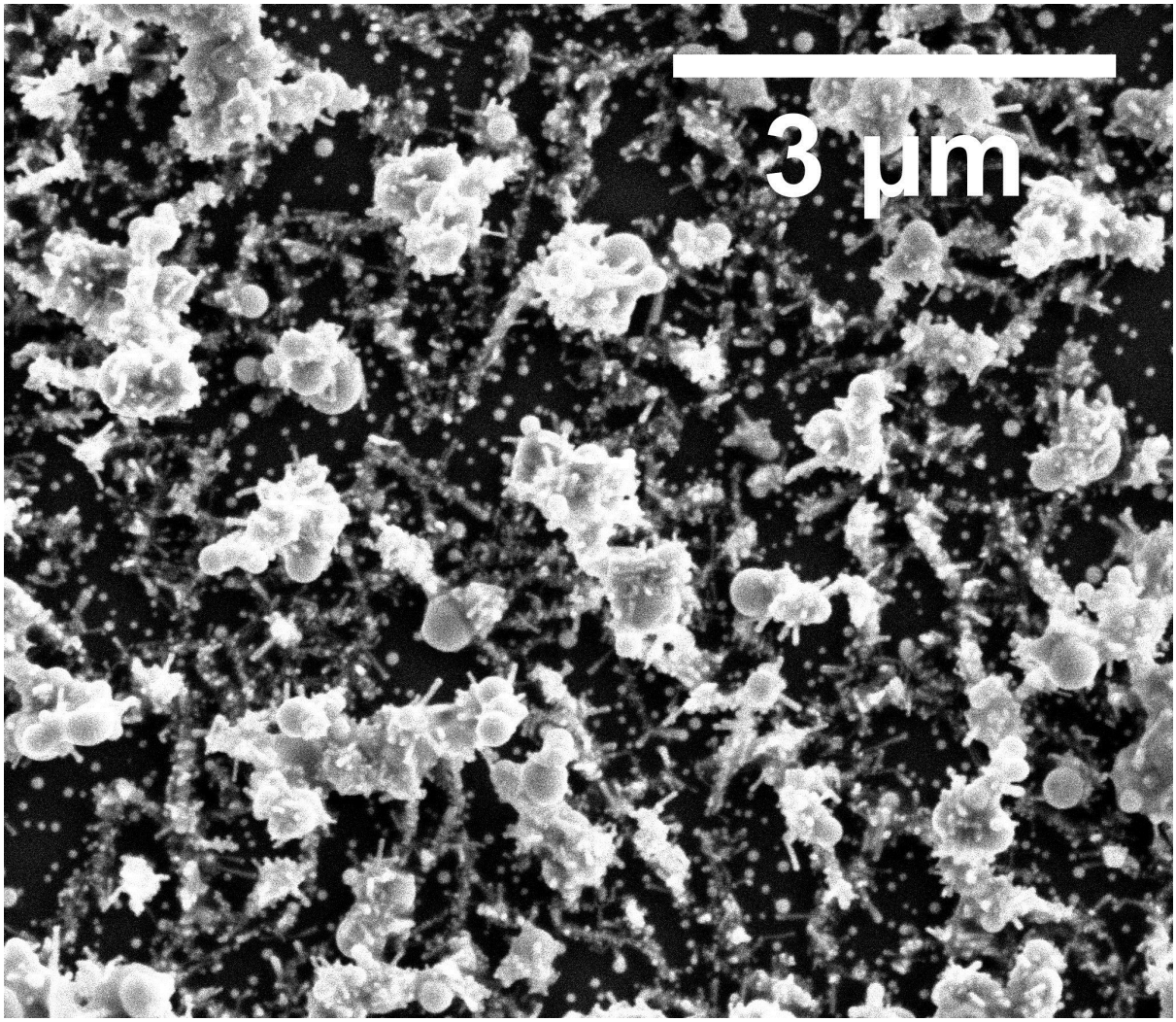


Figure S6: SEM (a) of $Ge_{1-x}Sn_x$ nanowires grown with TET as the Sn source at 470 °C. EDX analysis revealed an erratic amount of Sn incorporation from one nanowire to another (*i.e.* 4 – 8 at. % Sn).

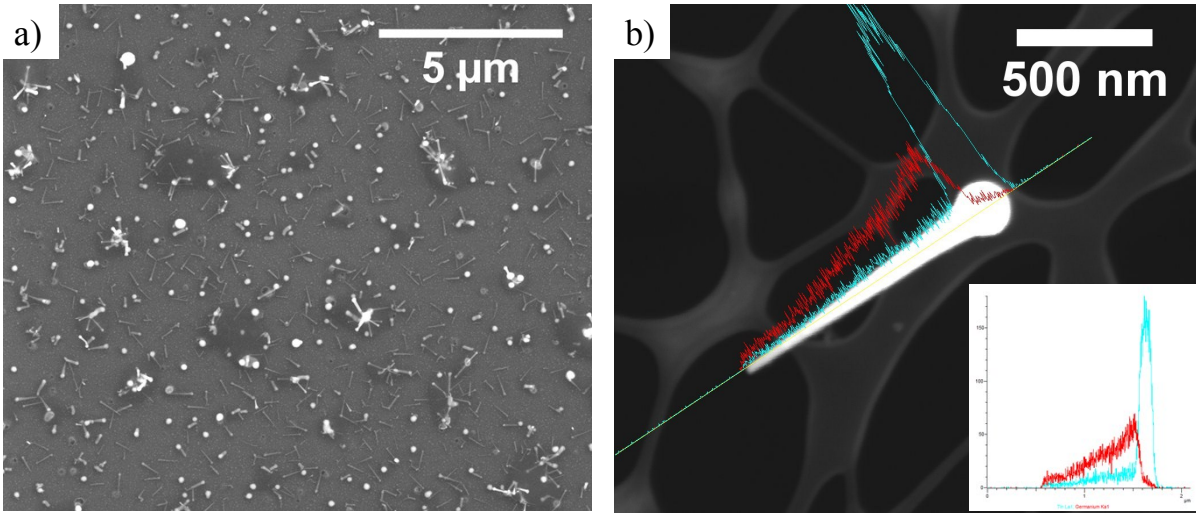


Figure S7: $Ge_{1-x}Sn_x$ nanowires catalysed by $Au_{0.70}Ag_{0.30}$ nanoparticles with ~11 at. % Sn. The low yield of these nanowires is apparent from (a), the $Ge_{1-x}Sn_x$ nanowires are sporadic clusters across the substrate. A STEM image (b) shows the severe tapering of these nanowires from tip to end. The linescan in (b) reveals that the Sn content of the nanowire is also inconsistent along the bulk of the nanowire, with more Sn incorporation in the wider diameter area of the nanowire, closer to the seed. The EDX point measurements were taken approximately 200 nm from the seed to compensate for this inconsistency.

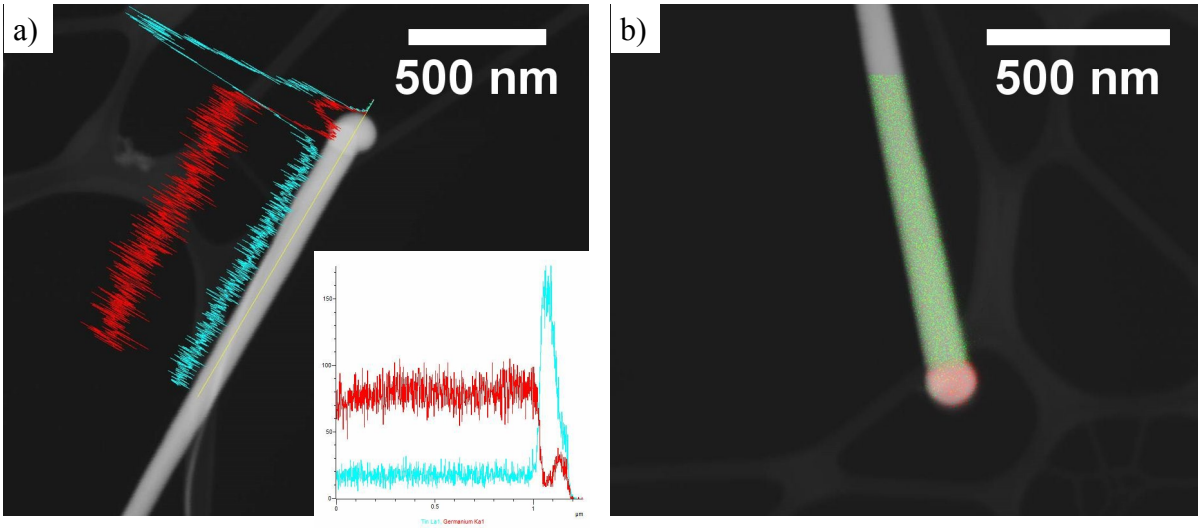


Figure S8: EDX analysis of $Ge_{1-x}Sn_x$ nanowires catalysed by $Au_{0.80}Ag_{0.20}$ nanoparticles with 9.14 at. % Sn. In the linescan (a) Ge is denoted by red and Sn by blue. In the elemental map (b) Ge is denoted by Green and Sn by red. The Sn rich nature of the seed and lack of Sn clustering and segregation is apparent from the linescan in (a) and the elemental map in (b).

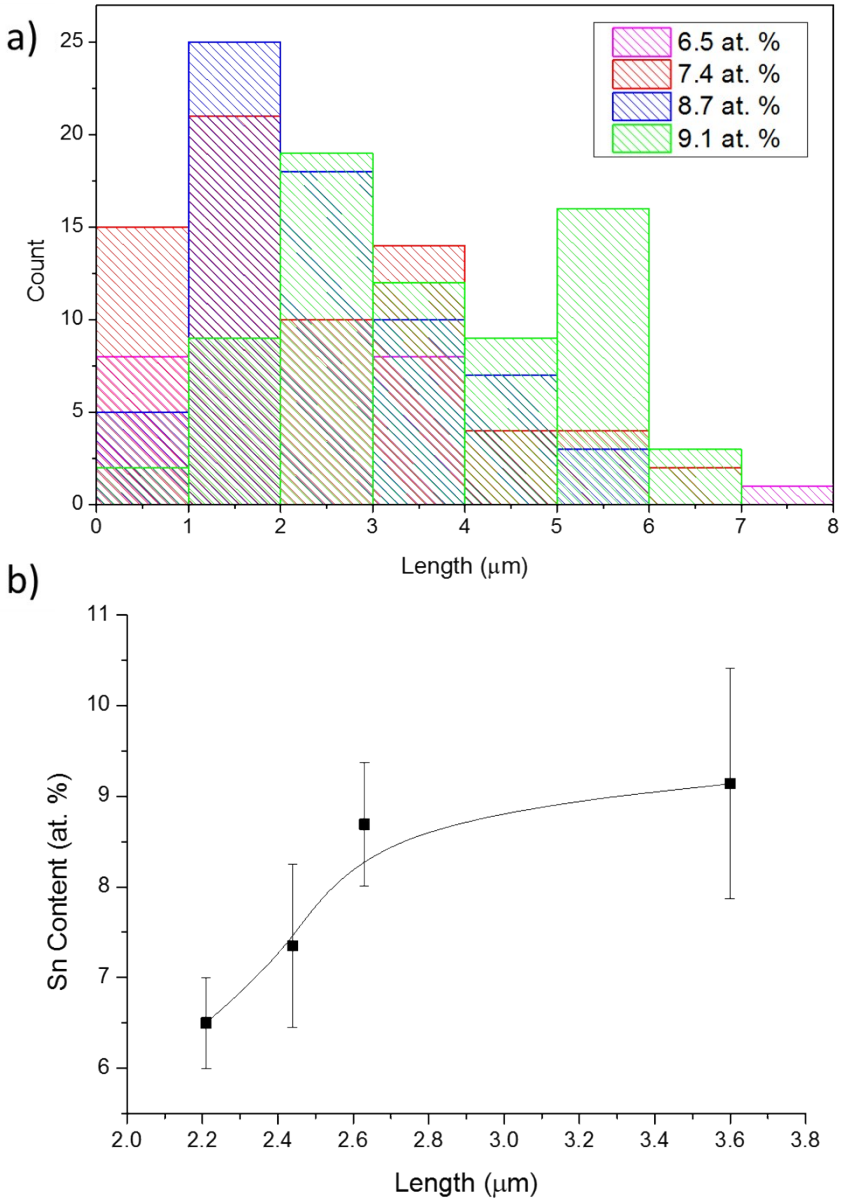


Figure S9: The length distributions (a) of $Ge_{1-x}Sn_x$ nanowires with varying Sn content, ranging from 6.5 at. % Sn, fabricated with ATBS as Sn source and $Au_{0.90}Ag_{0.10}$ nanoparticles as catalyst, to 9.1 at. % Sn, obtained using TET as Sn source and $Au_{0.80}Ag_{0.20}$ nanoparticles as catalyst. (b) Displays the relationship between mean Sn content and mean length, the error bars here represent the standard deviation from the mean Sn content.

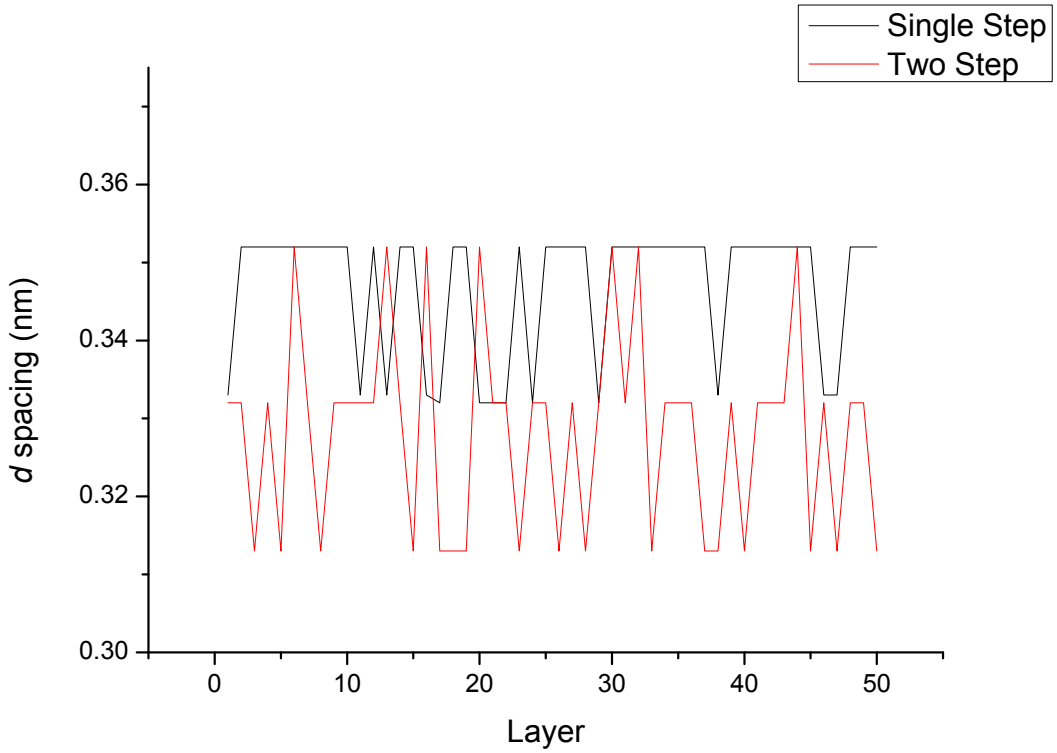


Figure S10: Comparison of the interplanar (*d*) spacing of 50 successive layers of $Ge_{1-x}Sn_x$ nanowires. The black line denotes the nanowires fabricated through increased growth kinetics with 9.1 at. % Sn, while the red line represents nanowires grown using a two-step method with 9.2 at. % Sn.

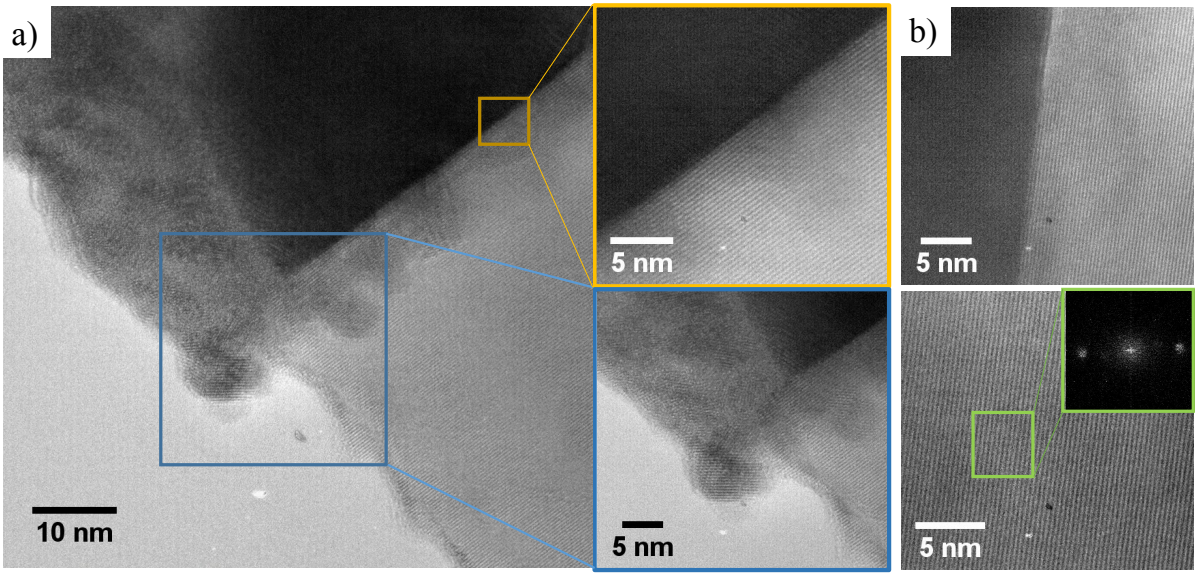


Figure S11: TEM analysis of $Ge_{1-x}Sn_x$ nanowires with 9.1 at. % Sn. The sharp interface between the nanowire seed and body is clearly seen in (a), in the orange coloured box, and (b). There is no segregation of metallic Sn apparent at the interface. Also visible is the less Sn rich "bulb" surrounding the Sn rich seed (blue coloured box). These nanowires were defect free with no apparent stacking faults of twin boundaries and display <111> as the dominant growth direction.

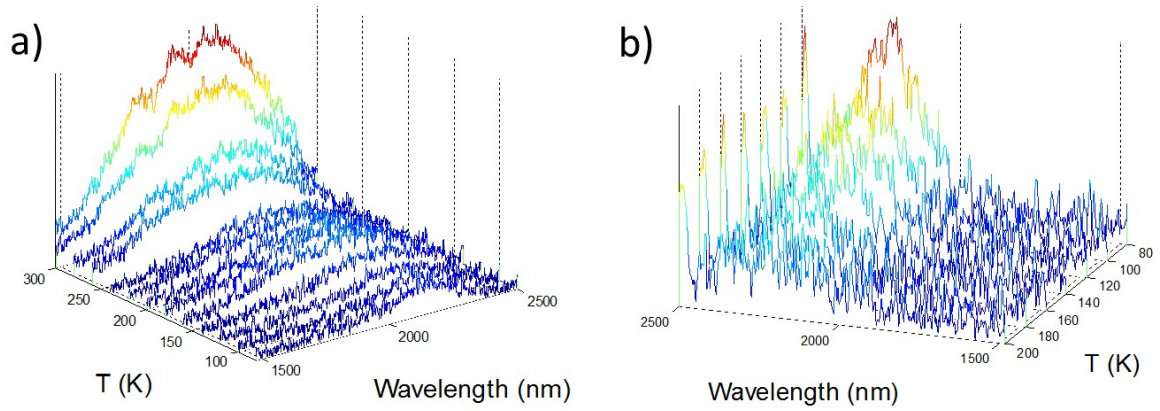


Figure S12: Temperature dependent photoluminescence studies in part (a) and (b) convey the different behaviours of the $Ge_{1-x}Sn_x$ nanowires with 7.4 and 9.1 at. % Sn respectively. In (a), the dominance of indirect transitions at low temperature with this Sn content is observed. The temperature dependent PL displays an increase of intensity with increasing temperature; indicative of an indirect bandgap material. In (b), the contrary is observed – due to dominance of indirect transitions at low temperature with this Sn content ($x = 0.09$) an inverse relationship exists between temperature and PL intensity. In terms of absolute intensity, $Ge_{1-x}Sn_x$ nanowires with 7.4 at. % Sn have a maximum intensity of 1.29 E-4, while the 9.1 at. % Sn sample has a maximum intensity of 3.83 E-5.

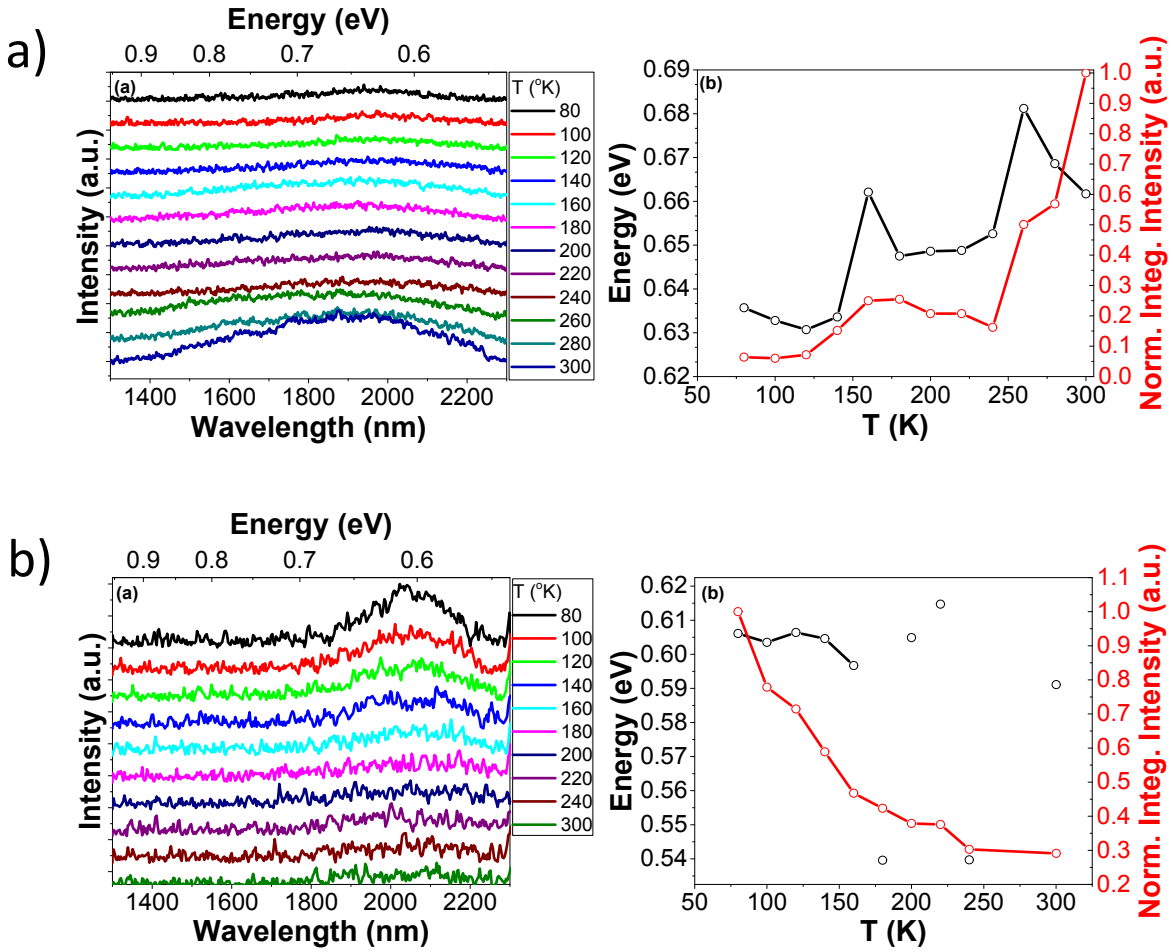


Figure S13: Temperature dependent photoluminescence studies in part (a) and (b) convey the different behaviours of the $Ge_{1-x}Sn_x$ nanowires with 7.4 and 9.1 at. % Sn respectively. They also display the shift in energy and integrated intensity as a function of temperature.

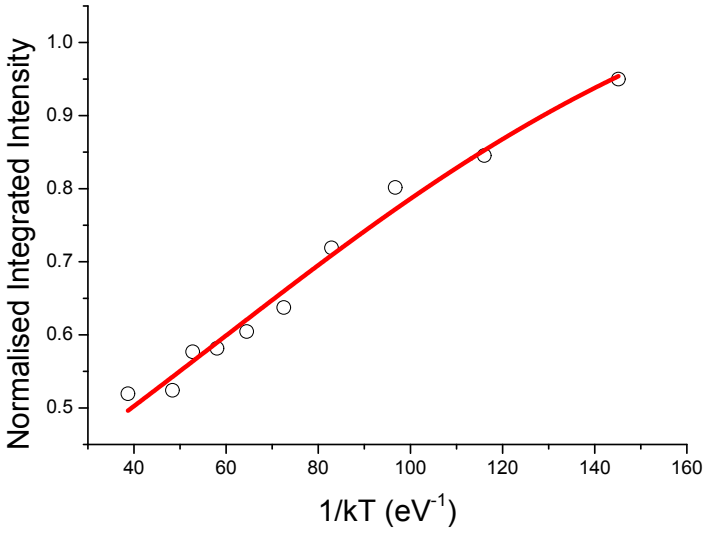


Figure S14: Arrhenius plot for the $Ge_{1-x}Sn_x$ nanowires with $x = 0.09$ at low temperature. The red line represents the Arrhenius fit, which gave an activation energy of $E_A = 16$ meV.

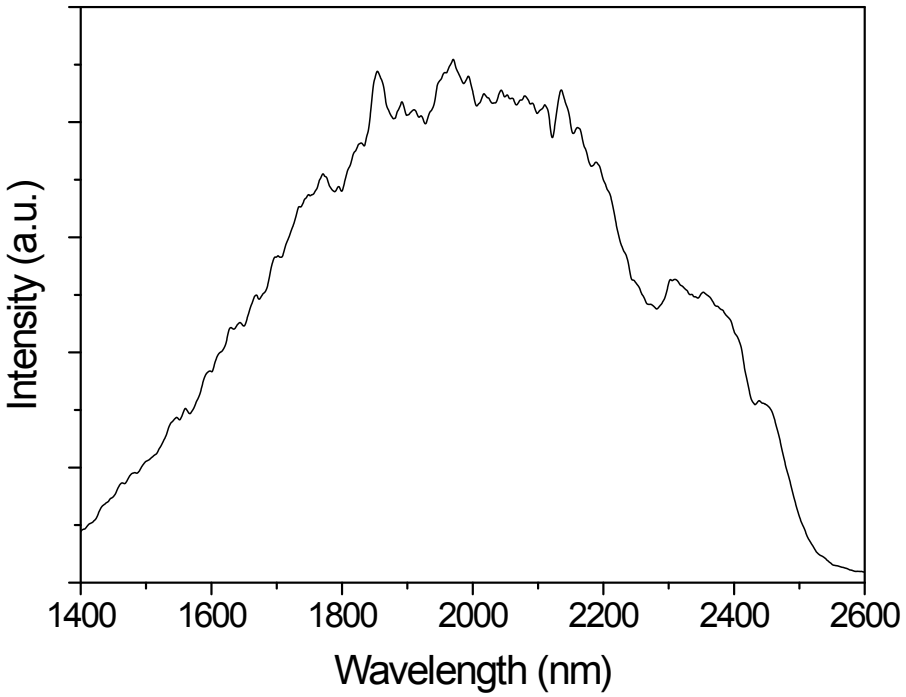


Figure S15: Photoluminescence spectra of 9.2 at. % Sn sample fabricated through a two-step process. The peak has a broad FWHM of 761 nm, centred at 1988 cm (0.62 eV).



Figure S16: Enlarged view of the sub 1.0 eV region of the EELS Spectra. The bandedge can be clearly seen at approx. 0.61 – 0.62 eV.